Thermochimica Acta, 241 (1994) 199–212
Elsevier Science B.V., Amsterdam
SSDI 0040-6031(93)01674-R

XRD, spectroscopic and thermal analysis studies on 3-nitro-1,2,4-triazole-5-one (NTO)

K.V. Prabhakaran [a], S.R. Naidu [b] and E.M. Kurian [b,]*

[a] *Armament Research and Development Establishment, Pashan, Pune-411 021, India*

[b] *Explosive Research and Development Laboratory (Defence Res. & Dev. Orgn.), Ministry of Defence, Armament Post, Sutarwadi, Pune-411 021, India*

(Received 30 July 1993; accepted 12 December 1993)

Abstract

The kinetics and mechanism of the thermal decomposition of 3-nitro-1,2,4-triazole-5-one (NTO), a heterocyclic nitro triazole, have been studied, together with its morphology and evolved gaseous products, using thermogravimetry (TG), differential thermal analysis (DTA), infrared spectroscopy (IR), differential scanning calorimetry (DSC), X-ray diffractometry (XRD) and hot-stage microscopy. The crystal structure parameters obtained from the XRD pattern are $a = 20.000 \pm 0.005$ Å, $b = 20.000 \pm 0.005$ Å, and $c = 6.573 \pm 0.005$ Å. The crystal belongs to the tetragonal system, with a c/a ratio of 0.329.

The IR spectrum of NTO has also been recorded and the bands assigned. The kinetics of the thermolysis has been followed by both isothermal TG and IR. The best linearity, with a correlation coefficient of 0.9937, was obtained for the Avrami–Erofe'ev equation, $n = 3$, in the range 0–83% α, using isothermal TG. The activation energy was found to be 186 kJ mol^{-1}, with $\log(A/\mathrm{s}^{-1})$ being 16.64. The effect of a series of additives, incorporated to an extent of 5%, on the initial thermolysis of NTO has also been studied. Evolved gas analysis by IR showed that CO_2, NO_2, NO and N_2O are produced in larger amounts than CO and HCN. The cleavage of the C–N bond appears to be the primary step in the thermolysis of NTO.

INTRODUCTION

Syntheses of high-energy materials of higher insensitivity [1] and high brisance are being studied vigorously in order to meet the superior performance requirements of hyper-velocity weapon application. The reported synthesis of 3-nitro-1,2,4-triazole-5-one (NTO) [1–3] represents an advance in this direction. Because of its high insensitivity, its ability to withstand very high mechanical and thermal shocks [1–6], its ease of manufacture from readily available chemicals by a simple nitration route, and its high velocity of detonation as compared to bicyclic nitro aromatics [7, 8], hexa-

---

* Corresponding author.

nitrostilbene [9], triamino trinitro benzene [10–13], 2-amino-4,6,7,9-tetranitro pyrimidine [14], 1,3,5,7-tetranitro adamantane [15], and the tetranitro derivative of dibenzo-1,3,4,6-tetraza pentaline [16–21], NTO appears to be a potential member of this class of high-energy materials. Rothgery et al. [22] have studied its thermokinetic behaviour using DSC, thermogravimetric analysis coupled with mass spectroscopy, and accelerating rate calorimetry, and have suggested that NTO decomposes via an autocatalytic mechanism. Xie et al. [23] have also studied the kinetics of the thermal decomposition of NTO using TG, DSC, IR and XRD by non-isothermal methods, and have reported an energy of activation of 520.3 kJ mol^{-1} for the exothermic decomposition of NTO. Menapace [24] studied the photochemical and thermochemical decomposition of NTO by electron paramagnetic resonance spectroscopy (EPR) and high-performance liquid chromatography (HPLC). The decomposition rate was found to be inversely proportional to the initial amount of NTO present in the 50 and 100 mg decompositions, with an activation energy of 369.6 kJ mol^{-1}. Oestmart et al. [25], using thermal and mass spectral data, suggested that the possible decomposition path is an elimination of NO_2 followed by decomposition of the azole ring. Thermal data that they obtained by chemiluminescence analysis have shown that the decomposition is governed by an activation energy of 170 kJ mol^{-1}. Thus the kinetic data reported are evidently at considerable variance. There has been speculation about the relationship between the exceptional thermal stability of these compounds and their molecular structure. Solid state properties appear to be as significant as chemical constitution in determining their stability with respect to their effective end use. In order to determine the complex reaction pathways in the thermal decomposition of NTO, which is not yet fully understood, the present work was initiated [26], using simultaneous DTA–TG, IR, DSC, XRD and hot-stage microscopy under optimised experimental conditions [26, 27].

EXPERIMENTAL

NTO was prepared in gram batches in the laboratory using methods in the literature [1–3]. EGA was carried out using a specially designed IR gas cell [26] fabricated from pyrex glass using pre-pelletted spectroscopic grade KBr windows under partial evacuation. Further experimental details are given in our previous communication [27].

RESULTS

IR spectra of NTO

Molecular orbital calculations [28] show that ^{1}H and ^{4}H tautomers are most stable in NTO. The IR spectrum of the methyl derivative of NTO has been reported [29]; however no band assignments are available. The IR

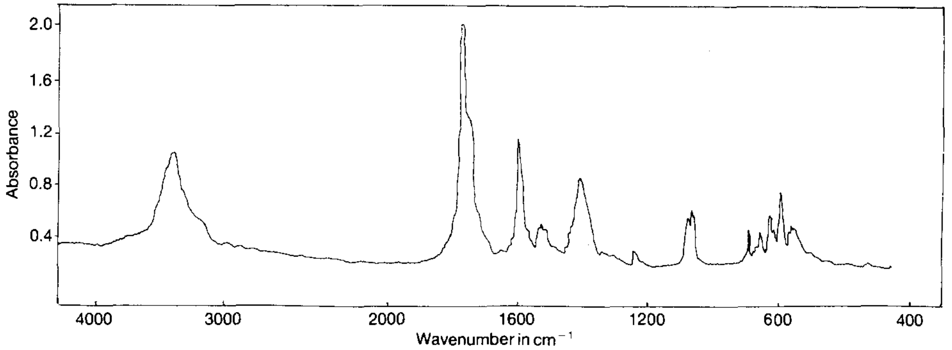

Fig. 1. IR spectrum of NTO.

TABLE 1

IR spectral assignments of NTO

Wavenumber/cm^{-1}	Assignment
3200s	ν(N–H)
1720s	ν(C=O) (unsaturated ring exo C=O)
1700sh	ν(C=N)
1550s	$\nu(NO_2)$, asym.
1470m	ν amide 2 (cis)
1360s	$\nu(NO_2)$, sym.
1280w	Amide 3
1190m	ν(N–N), ring
1020m	ν(C–N)
1010m	
830m	NO_2 deformation
790m	
760m	
740m	Amide 4 and 5
690m	
610m	

Key: m, medium; s, sharp; sh, shoulder; w, weak.

spectrum of NTO is given in Fig. 1, with band assignments in Table 1. NTO has the 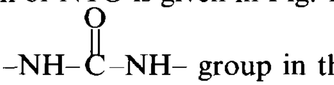 $-NH-\overset{O}{\overset{\|}{C}}-NH-$ group in the five-membered ring which gives rise to the characteristic carbonyl absorption band at 1720 cm^{-1}. This value is high when compared to the 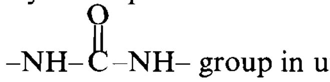 $-NH-\overset{O}{\overset{\|}{C}}-NH-$ group in urea (1680 cm^{-1}), because of the five-membered ring system. The band at 1700 cm^{-1} may be ascribed to the C=N stretching vibration. This higher value is possibly due to the substitution of the NO_2 group on the C=N. The bands at 1550, 1360 and 790 cm^{-1} can be assigned to the asymmetric and symmetric stretching, and deformation vibration of the NO_2 group, respectively. Most of the remaining bands can be assigned to various amide group vibrations. Thus the bands at 1470 and 1280 cm^{-1} can be ascribed to the amide 2 (cis) and amide 3 group vibrations. The bands at 740, 690 and 610 cm^{-1} can be assigned to the amide 4 and 5 groups.

XRD studies

XRD studies using the powder diffraction method show that the sample belongs to the tetragonal crystal system with a c/a axial ratio of 0.329 (Fig. 2 and Table 2).

Simultaneous thermal analysis

Simultaneous TG/DTA/DTG curves of NTO were recorded in static air as well as in dynamic nitrogen atmosphere at a heating rate of 5°C min^{-1}; and the thermograms obtained in dynamic nitrogen atmosphere are given in Fig. 3. The TG data indicate that NTO undergoes decomposition in two stages in the temperature ranges of 251-262°C and 262°C onwards. The weight loss observed for the sharp first stage is about 67%. The second stage is sluggish and faster in air than in nitrogen. The results obtained are similar when the heating rate was 10 and 20°C min^{-1}. In DTA, the first exotherm is very sharp and dominant and occurs in the temperature range 251-271°C. The DTA curve also displays a broad overall exotherm, being

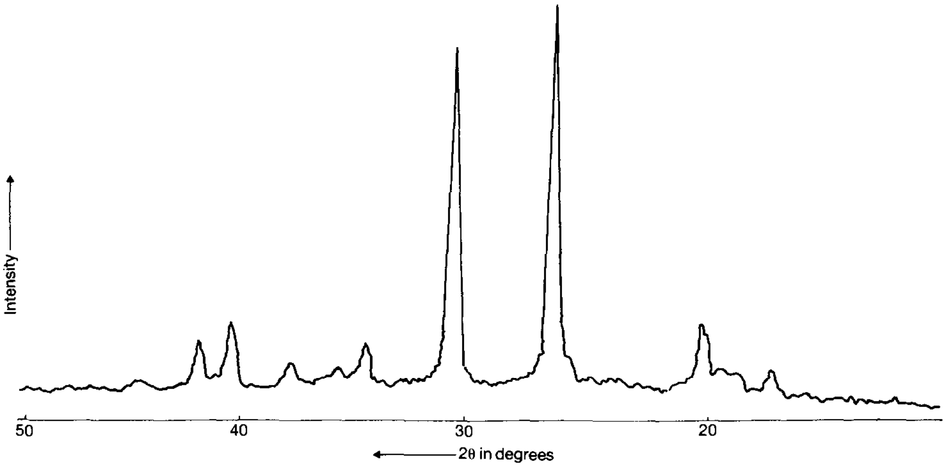

Fig. 2. XRD pattern of NTO.

TABLE 2

Intensities, d values and refined crystal data of NTO calculated from Bragg angle[a]

Line No.	Bragg angle θ/deg.	Intensity/%	d_{hkl}/Å	Exptl. $\sin^2\theta$	Calcd. $\sin^2\theta$	d_{hkl}
1	8.90	7	4.984	0.0239	0.0256	221
2	9.60	5	4.623	0.0278	0.0271	031/301
3	9.90	3	4.484	0.0256	0.0286	131/311
4	10.30	13	4.312	0.0320	0.0331	231/321
5	13.40	100	3.327	0.0537	0.0550	002
6	15.50	89	2.885	0.0714	0.0699	132
7	17.45	11	2.571	0.0899	0.0910	461/641
8	18.00	3	2.495	0.0955	0.0937	152/512
9	19.05	6	2.362	0.1065	0.1085	062/602
10	20.25	17	2.228	0.1198	0.1207	661
11	20.95	11	2.156	0.1278	0.1268	113

[a] $a = 20.000 \pm 0.005$ Å, $b = 20.000 \pm 0.005$ Å and $c = 6.573 \pm 0.005$ Å (c/a axial ratio $= 0.329$).

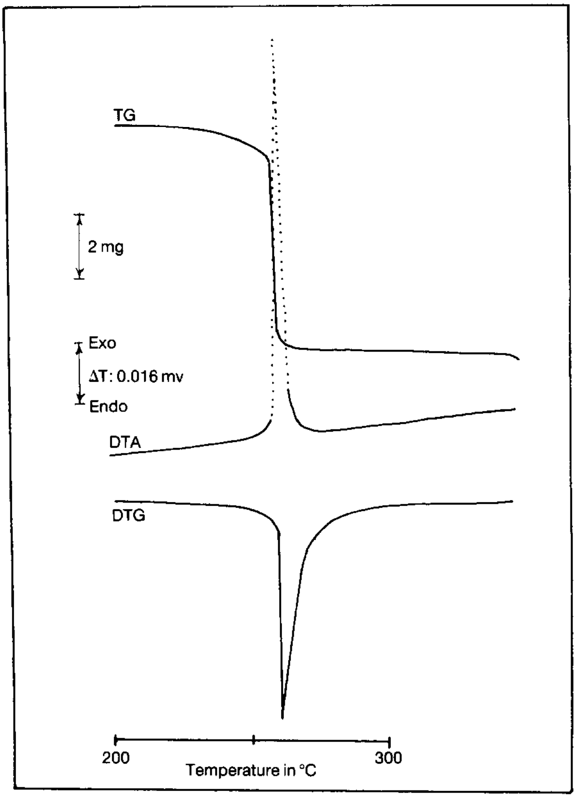

Fig. 3. TG/DTA/DTG curves of NTO. Sample weight, 10.0 mg; reference, calcined alumina; atmosphere, dynamic nitrogen (10 l h^{-1}).

established at about 271°C; this change is more dominant in static air than in nitrogen as expected, because it corresponds to oxidative degradation of the intermediates formed. The DTA does not show any endothermic tendency before the onset of the first exotherm, indicating that the compound decomposes without melting. The DSC curve shows a sharp exotherm setting in at 253°C. This exothermic change is covered by an energy change of 1331.2 J g^{-1}. The DSC curve also displays two weak exotherms at 335 and 504°C, respectively.

Effect of additives

The effect of added metal oxides/additives, incorporated to the extent of 5%, on the DTA profile of NTO was studied (Table 3). From these curves, the initial temperature of decomposition T_i, the temperature of the peak maximum T_m, and the final temperature of decomposition T_f were evaluated, and these, arranged in increasing order of the peak maximum temperature are given in Table 3. From this table, it can be concluded that:

(a) The temperature of the peak maximum of NTO is decreased by lead monoxide, cuprous oxide, monobasic lead stearate, cupric oxide, titanium dioxide, ferric oxide, magnesium oxide and zirconium dioxide, which indicates that they accelerate the thermolysis of NTO.

TABLE 3

Effect of additives on the initial thermolysis of NTO

Additive	Temperature of decomposition/°C		
	T_i	T_m	T_f
Lead monoxide	251	254	273
Cuprous oxide	241	254	273
Monobasic lead stearate	210	255	274
Cupric oxide	245	257	273
Titanium dioxide	229	257	274
Zirconium dioxide	255	258	286
Ferric oxide	226	259	268
Magnesium oxide	190	261	271
NTO	241	262	292
Copper chromite	247	264	295
Lanthanum oxide	264	268	292
Monobasic copper stearate	247	268	291
Nickel oxide	262	269	295
Cerium oxide	257	271	289
Cobaltic oxide	270	274	301
Thorium oxide	264	276	298

(b) Copper chromite, lanthanum oxide, monobasic copper stearate, nickel oxide, cerium oxide, cobaltic oxide, and thorium oxide give higher T_m values indiating that they decelerate the thermolysis of NTO.

Kinetics by isothermal TG

The kinetics [30] of the isothermal decomposition of NTO was studied at different temperatures in the temperature range 229–246°C under static air atmosphere. The $\alpha-t$ relationship was sigmoidal in nature. From the data obtained, the fraction decomposed α at a given time t was evaluated. To evaluate the rate constants, the $\alpha-t$ curve (Fig. 4) was analysed for various kinetic expressions listed in Table 4 of our previous communication [27] using a computer program developed for this purpose. The rate constants obtained from the slopes of the plots of these equations were substituted in the Arrhenius equation to determine the kinetic parameters. Out of the eighteen equations tried, close correlation was observed for six; these are reproduced in Table 4 with the corresponding rate parameters obtained. The best linearity, with a correlation coefficient of 0.9937, was, however, obtained for the Avrami–Erofe'ev equation, $[-\ln(1-\alpha)]^{1/3}$, for an α range of 0–83%, which gave an activation energy of 186.0 kJ mol^{-1} and a $\log(A/\text{s}^{-1})$ value of 16.64; these are considered to be the best values. Good

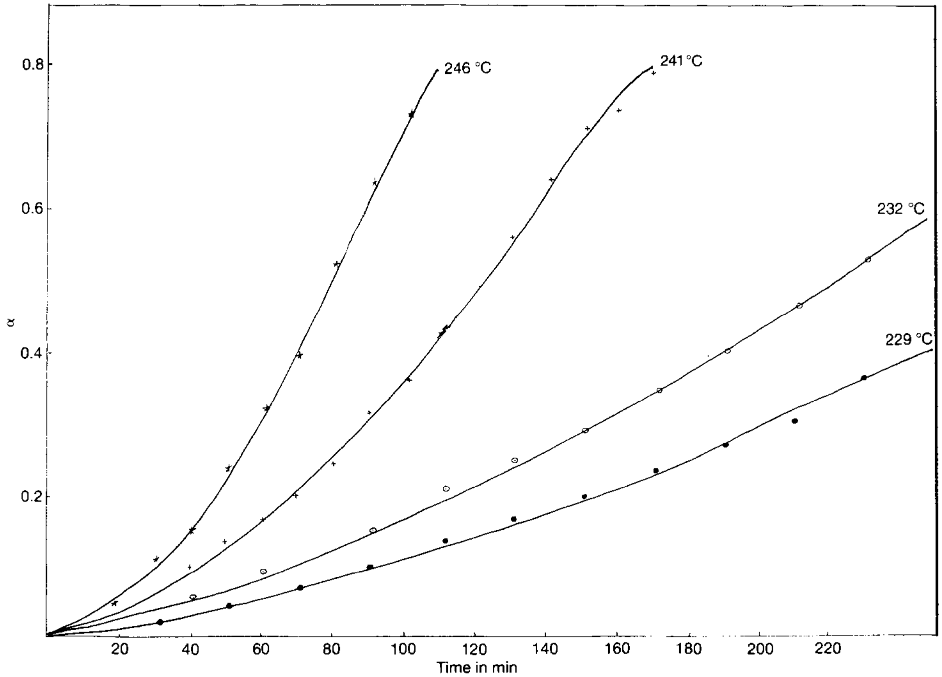

Fig. 4. $\alpha-t$ plots for the thermal decomposition of NTO (TG).

TABLE 4

Correlation coefficient r obtained for various $f(\alpha)$ by iso-TG

$f(\alpha)$	r at isothermal temperatures/°C				E/kJ mol^{-1}	log(A/s^{-1})
	229	232	241	246		
$\alpha^{1/2}$	0.9931	0.9846	0.9887	0.9936	174.0	15.42
$[-\ln(1-\alpha)]$	0.9559	0.9316	0.9240	0.8942	228.0	21.18
$[-\ln(1-\alpha)]^{3/2}$	0.9898	0.9825	0.9765	0.9641	205.0	18.73
$[-\ln(1-\alpha)]^{1/2}$	0.9956	0.9940	0.9922	0.9878	195.0	17.62
$[-\ln(1-\alpha)]^{1/3}$	0.9918	0.9906	0.9949	0.9976	186.0	16.64
$[-\ln(1-\alpha)]^{1/4}$	0.9859	0.9818	0.9898	0.9958	181.0	16.11

correlation was observed between the kinetics of the initial thermolysis and the velocity of detonation in the case of NTO (Fig. 9 in ref. 27).

Kinetics by IR spectroscopy

In the IR spectra, the variation in the intensity of the nitro band at 1550 cm^{-1} (Fig. 1 and Table 1) was used to monitor the decomposition, using a loose-mix method [27] in the temperature range 195–210°C.

The $\alpha - t$ curves thus obtained (Fig. 5) were analysed using the various rate equations, as in the iso-TG, to evaluate the rate constants. Six rate

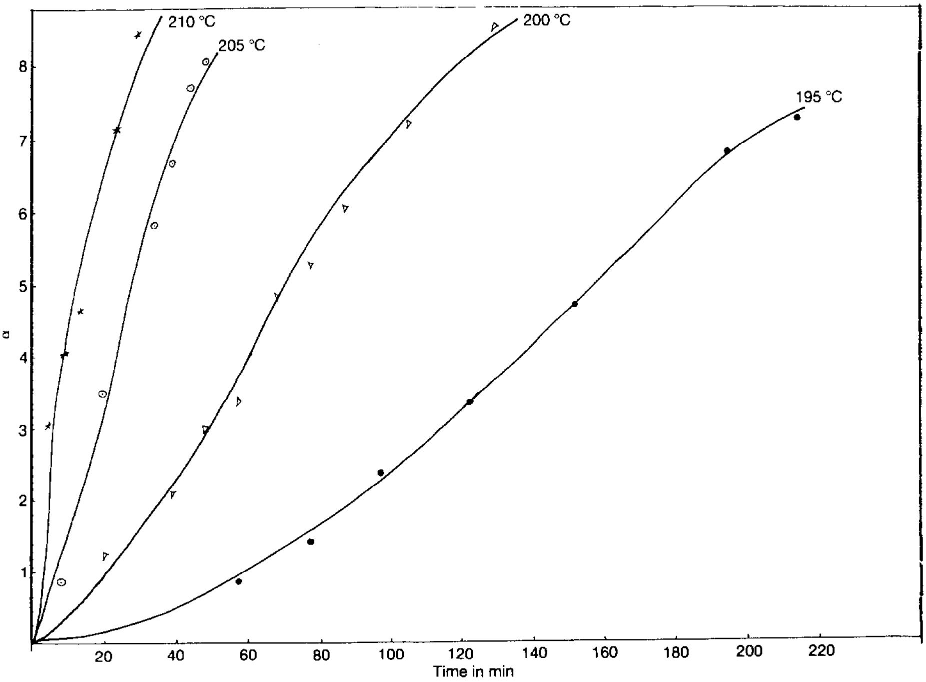

Fig. 5. $\alpha - t$ plots for the thermal decomposition of NTO (IR).

TABLE 5

Correlation coefficient r obtained for various $f(\alpha)$ by iso-IR

$f(\alpha)$	r at isothermal temperatures/°C				E/kJ mol^{-1}	$\log(A/\mathrm{s}^{-1})$
	195	200	205	210		
$1-(1-\alpha)^{1/2}$	0.9920	0.9635	0.9952	0.8704	231.0	23.24
$1-(1-\alpha)^{1/3}$	0.9930	0.9468	0.9884	0.8552	236.0	23.71
$[-\ln(1-\alpha)]^{3/2}$	0.9950	0.9531	0.9870	0.8569	233.0	23.81
$[-\ln(1-\alpha)]^{1/2}$	0.9896	0.9724	0.9911	0.8742	224.0	22.82
$[-\ln(1-\alpha)]^{1/3}$	0.9763	0.9841	0.9811	0.8903	206.0	20.66
$[-\ln(1-\alpha)]^{1/4}$	0.9664	0.9870	0.9705	0.8979	211.0	21.09

equations which gave higher correlation coefficients are reproduced in Table 5 with the corresponding rate parameters. The best linearity, with a correlation coefficient of 0.9580, was, however, obtained for the Avrami–Erofe'ev equation, $[-\ln(1-\alpha)]^{1/3}$, and this was used for the evaluation of the rate parameters. The activation energy was found to be 206.0 kJ mol^{-1} with a $\log(A/\mathrm{s}^{-1})$ value of 20.66. The difference in the rate parameters arrived at by TG and IR may be due to the fact that the TG data pertain to global kinetics whereas the IR data are specific to the nitro group and are perhaps also influenced by the matrix.

Evolved gas analysis by IR

In order to get an insight into the mechanism of the thermal decomposition, the gaseous species evolved when 10 mg of the sample was decomposed at a controlled heating rate of 10°C min^{-1} were examined and identified using IR spectroscopy. At around 244°C, carbon dioxide and nitrous oxide were the first gases that could be detected. The gaseous species identified (Fig. 6) are given in Table 6. The bands due to CO_2, NO_2 and N_2O are very prominent in the spectra.

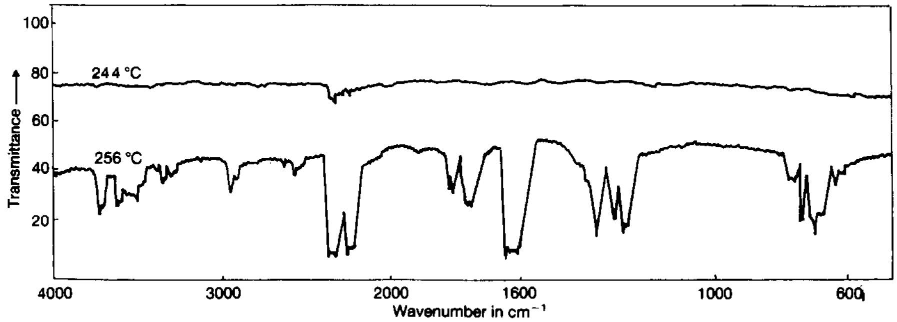

Fig. 6. IR spectra of the gaseous decomposition products of NTO.

TABLE 6

Gaseous thermolysis products of NTO: IR spectra

Gaseous species	Wavenumber/cm^{-1}		Gaseous species	Wavenumber/cm^{-1}	
	Reported	Observed		Reported	Observed
Nitrogen dioxide	1730st	1750	Nitrous oxide	2565m	2560
	1625st	1630		2220st	2220
		1610		1310st	1310
	1258st	1270		1250st	1250
	754st	760	Nitric oxide	1840m	1820
Carbon dioxide	2340st	2340		1760m	1790
	720m	720	Hydrogen cyanide	3246st	3280
	666st	660		1379st	1380
Carbon monoxide	2140	2120		720	720
	2127m	2120			

Key: m, medium; st, strong.

Microscopic studies

At normal temperatures, the crystals are transparent; the transparency gradually decreases as the temperature increases. At about 230°C, the crystals start to disintegrate and gas evolution sets in, increasing in intensity at localised points. With increasing intensity, fogging occurs and finally a black charred residue is left.

DISCUSSION

The TG/DTA results (Fig. 3) indicate that the thermal decomposition of this compound proceeds basically in two stages. The first stage is more dominant and rapid, and involves about 67% loss in weight. The second stage is gradual and slower and involves about 23% loss in weight. The DTA curve shows corresponding exothermic changes. The first exotherm is very sharp. Isothermal TG, however, indicates that the change in weight up to 83% apparently takes place in one stage.

When the sample was pelleted in KBr, the decomposition was complete in 155 min at 210°C. The same behaviour was noted in other matrix materials such as KCl and NaCl. When it was loosely mixed with KBr powder the decomposition was over in just 45 min at 210°C. This shows that matrix consolidation influences the decomposition. The deceleration in decomposition on consolidation into pellet form is perhaps due to diffusional resistance to the escape of product gases from the reaction interface.

In the loose mixture method, the IR bands due to the nitro group initially decreased in intensity faster than those due to other groups. Also new bands

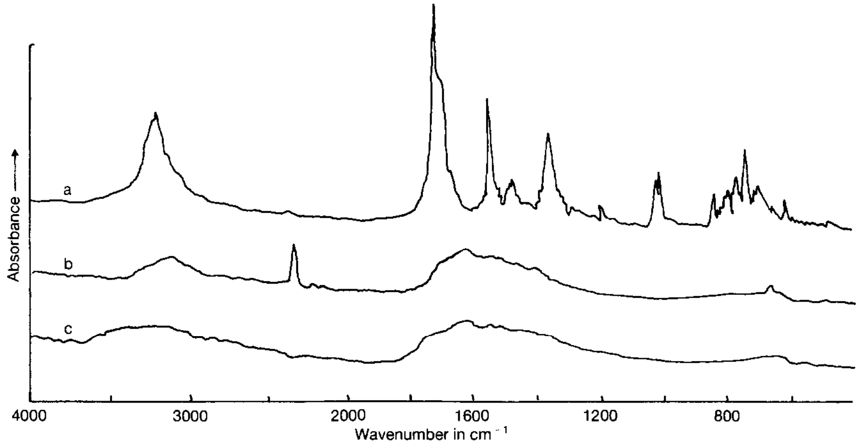

Fig. 7. IR spectra of NTO: curve a, at 185°C in KBr pellet; curve b, after 155 min at 210°C in KBr pellet; curve c, residue obtained after 83% loss in weight in iso-TG.

were observed at 3420, 1630 and 1530 cm^{-1} which are best assigned to a trans amide group (see Exhibit 1).

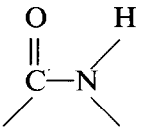

Exhibit 1. The transamide group.

When the thermal decomposition of the sample was followed by the IR method in KBr pellet form, the band intensities due to the nitro and other groups decrease but also new bands 2340 and 2220 cm^{-1} are observed (Fig. 7), in addition to those observed in the loose-mix method. These new bands can be ascribed to species, such as CO_2 (2340 cm^{-1}) and N_2O (2220 cm^{-1}), trapped in the matrix.

In the evolved gas analysis, carbon dioxide and nitrous oxide were the first gaseous decomposition products detected. Subsequently, nitrogen dioxide, nitric oxide, carbon monoxide, and hydrogen cyanide were also observed. From a perusal of the intensities of the various bands, it seems that nitrous oxide, nitrogen dioxide, nitric oxide and carbon dioxide are the major decomposition products.

The spectra of the residues at the end of the iso-TG and IR experiments are similar (Fig. 7), with broad bands in the 3400–3200 and 1680–1500 cm^{-1} regions that are characteristic of the amide group. It would appear that a stable fragment containing the amide group is formed in the decomposition.

The thermal decompositions of similar compounds have not been studied before. Brill and Oyumi [31] have studied the thermal decomposition of

1,4-dinitroglycoluril (DINGU) and 1,3,4,6-tetranitroglycoluril (TINGU), which have some similarity with NTO and have concluded that such compounds, without a CH_2 group straddled by an amino nitrogen, are strong NO_2 generators (see Exhibit 2).

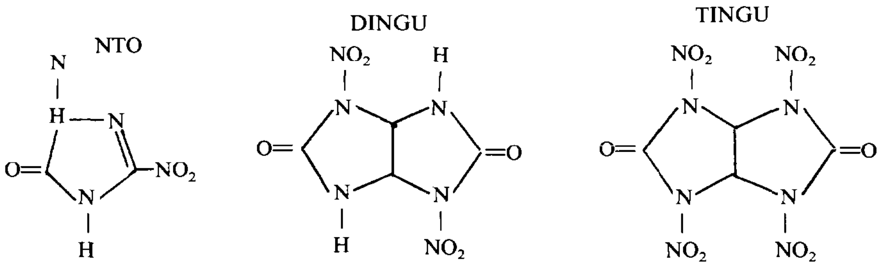

Exhibit 2. NTO, DINGU and TINGU.

They also noticed the formation of HNCO during the thermal decomposition but could not quantify it because the absolute IR intensities were not known. The decomposition behaviour of NTO closely resembles those of TINGU and DINGU, suggesting that after the breaking away of the NO_2 group in NTO the adjacent C–N bond is weakened and ruptures, giving rise to the amide group as shown in Exhibit 3.

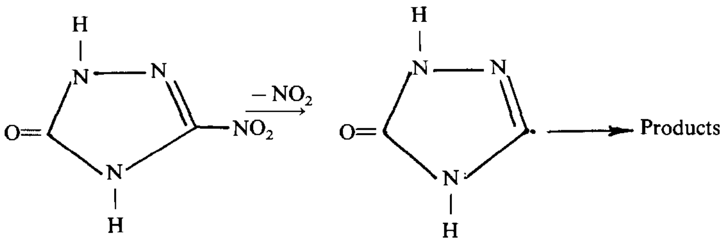

Exhibit 3. The decomposition of NTO.

These results can be rationalised by suggesting that C–NO_2 cleavage, with rupture of the adjacent C–N bond, appears to be the probable mechanism in the thermal decomposition of NTO and that this step is likely to be the rate-determining step. After rupture of the NO_2 group the ring will be quite unstable. Because the ring already has a C=N bond, adjacent to the C–NO_2 group, only the C–NH bond can break, giving rise to the trans amide fragment observed during the IR studies. The oxidative attack of the NO_2 group on the ring fragment accounts for the formation of products like CO_2, NO and N_2O.

Oyumi and Brill [32], Batt [33] and Gray [34] found that in C–NO_2 compounds, the C–NO_2 group rearranges to isomeric nitrates and that cleavage of the CO–NO bond is the initial pathway in the thermal decomposition. Richie et al. [35] using a Mindo/3 calculation have shown that the above mechanism is energetically possible. The decomposition pathways of NTO and the products thereof, with respect to the nitramines and aliphatic C–NO_2 compounds, are dependent on the concerned bond dissociation energies which are different in the present case. However the available evidence in the present study does not support the above mechanism as the rate-determining step, presumably due to the difference in the bond strengths [36] and molecular structural environments of the C–NO_2 group in NTO. However it is difficult to rule out completely such a mechanism as some NO is indeed found as a decomposition product.

The activation energy is in agreement with the mechanism suggested. Perusal of the kinetic parameters of various nitro alkanes, such as nitroethane and 1- and 2-nitropropane [37], shows that the thermal decomposition of these compounds is assumed to be by cleavage of the C–NO_2 bond and involves activation energies of 239.4, 231.0 and 226.8 kJ mol^{-1}, respectively, which are close to the value obtained in the present study. These results further confirm that C–NO_2 cleavage and subsequent rupture of the C–N bond resulting in the formation of the amide fragment appear to be the most probable initial mechanisms in the thermal decomposition of NTO.

REFERENCES

1 K.Y. Lee, L.B. Chapman and M.D. Coburn, J. Energ. Mater., 5 (1987) 27.
2 A. Becuwe, (Soc. Nat. des Poudres et Explo.), Fr., Demande FR. 2584066, (cl C06 B25/34) issued Jan. 2, 1987.
3 G. Cipens, R. Bokalders and V. Grinsteins, Khim. Geterotsikl. Soedin. Akad. Nauk Latv. SSR, 2 (1966) 110.
4 B.C. Beard and J. Sharma, J. Energ. Mater., 7(3) (1990) 181.
5 G. Zhou and G. Hong, Proc. Int. Pyrotech. Semin., 17(1) (1991) 276.
6 A. Finch, P.J. Gardner, A.J. Head and H.S. Majdi, J. Chem. Thermodyn., 23(12) (1991) 1169.
7 A.H. Blatt and A.W. Rytina, J. Am. Chem. Soc., 72 (1950) 403.
8 P. Golding and G.F. Hayes, Propellants Explos. Pyrotechnics, 4 (1979) 115.
9 K.G. Shipp, J. Org. Chem., 29 (1964) 2620.
10 H.H. Cady and A.C. Larson, Acta Crystallogr. Part 3, 18 (1965) 485.
11 J.R. Kolb and H.F. Rizzo, Propellants Explos. Pyrotechnics, 4 (1979) 10.
12 P.S. Makashir, Studies on the thermal decomposition of some nitro compounds, M.Sc. Thesis, University of Pune, 1985.
13 T. Urbanski, The Chemistry and Technology of Explosives, Vol. 4, Pergamon Press, Oxford, 1964, p. 202.
14 P.K. Dasgupta, A. Nayak, G.R. Newkomi and P.W. West, J. Org. Chem., 44 (1979) 2582.
15 E.E. Gilbert and G.P. Sollott, Chem. Eng. News, 58(4) (1980) 32.
16 R.A. Carboni and J.E. Castle, J. Am. Chem. Soc., 84 (1962) 2453.
17 R.A. Carboni, J.C. Kauer, J.E. Castle and H.E. Simmons, J. Am. Chem. Soc., 89 (1967) 2618.
18 R.A. Carboni, J.C. Kauer, W.R. Hatchard and H.J. Harder, J. Am. Chem. Soc., 89 (1967) 2626.

19 J.C. Kauer and R.A. Carboni, J. Am. Chem. Soc., 89 (1967) 2633.
20 Y.T. Chia and H.E. Simmons, J. Am. Chem. Soc., 89 (1967) 2638.
21 R.J. Harder, R.A. Carboni and J.E. Castle, J. Am. Chem. Soc., 89 (1967) 2643.
22 E.F. Rothgery, D.E. Audette, R.C. Wedlich and D. A. Csejka, Thermochim. Acta, 185 (1991) 235.
23 Y. Xie, R. Hu, X. Wang, X. Fu and C. Zhu, Thermochim. Acta, 189 (1991) 283.
24 J.A. Menapace, J. Phys. Chem., 95 (1991) 5509.
25 H. Oestmart, H. Bergman, G. Asqvist, A. Langlet and B. Persson, Proc. Int. Pyrotech. Semin., 16(1) (1991) 874.
26 K.V. Prabhakaran, Studies on the solid state reactivity of some cyclic nitro and nitrosamines, Ph.D. Thesis, University of Pune, 1990.
27 K.V. Prabhakaran, N.M. Bhide and E.M. Kurian, Thermochim. Acta, 220 (1993) 169.
28 J.P. Ritchie, J. Org. Chem., 54 (1989) 3553.
29 T.P. Kofman, M.S. Pevzner, L.N. Zhukova, T.A. Kravchenko and G.M. Frolova, Zh. Org. Khim., 16 (1980) 375 (in English).
30 E.M. Kurian, J. Therm. Anal., 35 (1989) 1111.
31 T.B. Brill and Y. Oyumi, Propellants, Explosives, Pyrotechnics, 13 (1988) 69.
32 Y. Oyumi and T.B. Brill, Combust. Flame, 62 (1985) 225.
33 L. Batt, in S. Patai (Ed.), Chemistry of Functional Groups, Wiley, New York, 1982, Suppl. F, p. 417.
34 P. Gray, Trans. Faraday Soc., 51 (1955) 1367.
35 J.P. Ritchie, M.J.S. Dewar and J. Alster, J. Org. Chem., 50 (1985) 1031.
36 C.F. Melius, in S.N. Bulusu (Ed.), Chemistry and Physics of Energetic Materials, Kluwer Academic Publishers, Boston, 1990, p. 31.
37 T. Urbanski, The Chemistry and Technology of Explosives, Vol. 4, Pergamon Press, Oxford, 1964, p. 226.